

# Fading features found in the kinematics of the far-reaching Milky Way stellar halo

Sarah A. Bird<sup>1,2★</sup> and Chris Flynn<sup>3</sup>

<sup>1</sup>Key Laboratory for Research in Galaxies and Cosmology, Shanghai Astronomical Observatory, Chinese Academy of Sciences, 80 Nandan Road, Shanghai 200030, China

<sup>2</sup>Tuorla Observatory, Department of Physics and Astronomy, University of Turku, Väisäläntie 20, FI-21500 Kaarina, Finland

<sup>3</sup>Centre for Astrophysics and Supercomputing, Swinburne University of Technology, Hawthorn, VIC 3122, Australia

Accepted 2015 June 26. Received 2015 June 25; in original form 2014 December 2

## ABSTRACT

We test the long-term kinematical stability of a Galactic stellar halo model, due to Kafle et al. (2012), who study the kinematics of approximately 5000 blue horizontal branch stars in the Sloan Digital Sky Survey. The velocity dispersion  $\sigma$  and anisotropy parameter  $\beta$  of the stars have been determined as functions of Galactocentric radius, over the range  $6 < R_{GC} < 25$  kpc, and show a strong dip in the anisotropy profile at  $R_{GC} \sim 17$  kpc. By directly integrating orbits of particles in a 3D model of the Galactic potential with these characteristics, we show that the  $\sigma$  and  $\beta$  profiles quickly evolve on a time-scale of a few  $\times 10$  Myr whereas the density  $\rho$  profile remains largely unaffected. We suggest that the feature is therefore transient. The origin of such features in the Galactic halo remains unclear.

**Key words:** stars: horizontal branch – stars: kinematics and dynamics – Galaxy: halo – Galaxy: kinematics and dynamics – galaxies: individual: Milky Way.

## 1 INTRODUCTION

Studying the Milky Way’s stellar halo is an important route to understanding galaxy formation, as the halo is such an old Galactic component. Intrinsically bright stars with easily measured radial velocities have been the usual means of doing so, with red giants and horizontal branch stars as typical tracers in such studies. Early studies of the stellar halo kinematics date to the 1950s, and focused on halo stars passing through the Solar neighbourhood, but it was not until the 1980s that large ( $\gtrsim 100$ ) samples of halo stars tens of kpc from the Sun began to be collected and analysed (see the reviews by Sandage 1986; Helmi 2008).

Milky Way halo BHB stars from  $\sim 5$  to 50 kpc have been studied by Sommer-Larsen, Flynn & Christensen (1994). They used about 100 stars to develop a kinematical model of the outer Milky Way halo, with the surprising result that the orbits of stars in the far outer halo ( $>20$  kpc) appear to be much more tangential than radial. Flynn, Sommer-Larsen & Christensen (1996) used simulations of such stars orbiting in the Milky Way potential which showed such a distribution of halo orbits is stable over a Hubble time.

Since then, numerous studies have added to the sample of BHB halo stars (Sommer-Larsen et al. 1997; Sirko et al. 2004; Deason, Belokurov & Evans 2011; Deason et al. 2012) but show a wide spread in the resulting kinematical models for the outer stellar halo.

Sommer-Larsen et al. (1997) analysed about 700 BHB stars, mainly within 20 kpc of the Sun, but also probing out to 50 kpc. They found that the outer stellar halo velocity dispersion (at  $\approx 50$  kpc) was quite ‘cold’ (i.e. low velocity dispersion), nearing  $100 \text{ km s}^{-1}$  compared with the value at the sun  $\simeq 140 \text{ km s}^{-1}$ . They concluded that outer halo orbits must be quite tangential (with a tangential velocity dispersion of about  $150 \text{ km s}^{-1}$ ), given the observed density distribution of halo stars and assumptions about the Milky Way’s dark matter distribution.

On the other hand, Sirko et al. (2004) have advocated an isothermal outer halo ( $R_{GC} \gtrsim R_{\odot}$ ), in which all three components of the velocity dispersion are  $\approx 100 \text{ km s}^{-1}$ , based on  $\approx 1200$  BHB stars from Sloan Digital Sky Survey (SDSS). Thom et al. (2005) subsequently analysed 530 BHB stars with radial velocities and distances from the Hamburg/ESO survey, finding it difficult to discriminate between the simplest, isothermal kinematic models and anything more complex, and advocating further studies of the inner halo to help resolve the issue.

Very distant BHB stars have recently been shown by Deason et al. (2011) and Deason et al. (2012) to have very ‘cold’ kinematics – low velocity dispersions of  $\approx 50\text{--}60 \text{ km s}^{-1}$  in the radial range 100 to 150 kpc. The density falloff in these regions is much steeper than inside 100 kpc, and the dynamical times rather long, so the region is unlikely to be well mixed. Comparison with the kinematical models of the inner region, which implicitly assume the halo is well mixed, are thus difficult.

More recently, Kafle et al. (2012) have used the Xue et al. (2011) catalogue of  $\approx 5000$  BHB halo stars found from Sloan Extension

\* E-mail: sarbir@utu.fi

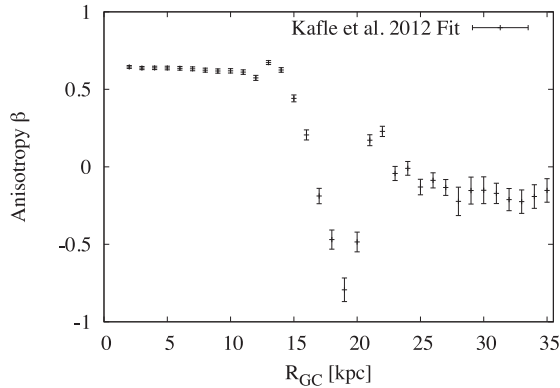


**Figure 1.** Anisotropy  $\beta$  profile as a function of Galactocentric radius,  $R_{GC}$ , showing  $\beta$  as calculated from the input Kafle et al. (2012) radial and tangential velocity dispersions,  $\sigma_r$  and  $\sigma_t$ . Kafle et al. (2012) measured the anomalous feature at its extremum to be  $\beta = -1.2$  at  $R_{GC} = 17$  kpc. The error bars are Poissonian.

for Galactic Understanding and Exploration-2 (SEGUE-2), part of the eighth data release of SDSS (Aihara et al. 2011), to analyse the kinematics of the Galactic stellar halo. Working from photometric distance estimates and radial velocity measurements for each star, they performed a maximum likelihood analysis to determine the velocity dispersion  $\sigma$  and anisotropy  $\beta$  profile, where  $\beta$  is defined by Binney & Tremaine (2008) in spherical coordinates using radial  $\sigma_r$  and tangential ( $\sigma_\theta, \sigma_\phi$ ) velocity dispersions such that

$$\beta = 1 - \frac{\sigma_\theta^2 + \sigma_\phi^2}{2\sigma_r^2}. \quad (1)$$

Kafle et al. (2012) found a previously unseen feature, most prominent in the  $\beta$  profile measured out to a Galactocentric radius of  $R_{GC} \approx 25$  kpc, which shows a rapid decline at  $R_{GC} = 13$  kpc, reaching a minimum at  $R_{GC} = 17$  kpc, followed by a sharp rise within just a few kpc (Fig. 1). This feature has been confirmed in a very recent study of the halo with an even larger sample of stars by King et al. (2015).

Given that the feature is so narrow and deep, but is made up of stars in an otherwise ‘hot’ (i.e. high velocity dispersion) Galactic halo, we were motivated by the question of whether such a feature could be long-term stable or simply transient.

We have tested this by setting up simulations of the stars in the Milky Way potential, and determined the model’s stability over the order of a Hubble time, finding that it is transient, and dissolves away in just a few tens of Myr.

In Section 2, we describe our choice of potential to use for our simulations (Flynn et al. 1996), updating it to be consistent with the remarkable new constraints on the Galactic potential by Bovy & Rix (2013). In Section 3, we describe our simulations testing stability over time of the stellar halo density distribution  $\rho$ , the velocity dispersion  $\sigma$ , and anisotropy  $\beta$  profiles, motivated as such by the analysis of Kafle et al. (2012). We discuss our results and draw conclusions in Section 4.

## 2 GALACTIC POTENTIAL MODEL

We used a Milky Way potential model similar to that of Flynn et al. (1996). The potential consisted of the sum of three components, namely the potential due to the dark halo, a central component, and the disc. The dark halo potential was spherical with mass of order  $10^{12} M_\odot$  within 100 kpc. The central potential was modelled by

**Table 1.** Adopted parameters for the Galactic potential.

Component	Parameter	Value	Unit
Dark halo	$r_H$	15.0	kpc
	$M(R_{GC} \lesssim 100 \text{ kpc})$	$\sim 10^{12}$	$M_\odot$
Bulge/Stellar halo	$V_H$	220	$\text{km s}^{-1}$
	$r_{C1}$	2.70	kpc
	$M_{C1}$	3.0	$10^9 M_\odot$
Central comp.	$r_{C2}$	0.42	kpc
	$M_{C1}$	16	$10^9 M_\odot$
Disc	$b$	0.3	kpc
	$r_{D1}$	5.81	kpc
	$M_{D1}$	106	$10^9 M_\odot$
	$r_{D2}$	17.43	kpc
	$M_{D2}$	-45.8	$10^9 M_\odot$
	$r_{D3}$	34.86	kpc
	$M_{D3}$	5.24	$10^9 M_\odot$

the sum of a spherical bulge/stellar-halo and a spherical inner core potential. The disc potential itself consisted of three Miyamoto–Nagai potentials (Miyamoto & Nagai 1975). In this model, the disc has a scalelength of  $R_D = 2.2$  kpc, to be consistent with the measurements of Bovy & Rix (2013) from the kinematics of over 16 000 G-type dwarfs in the SDSS/SEGUE survey distributed between Galactocentric radii of  $5 < R_{GC}/\text{kpc} < 12$ . Our Galactic potential model parameters are listed in Table 1. The parameters have been set such that the rotation curve, i.e. circular velocity as a function of Galactocentric radius, is flat out to  $R_{GC} = 500$  kpc – i.e. the outer limit of our modelled halo (although we only analyse the stars within 100 kpc). We adopted the same parameters used by Kafle et al. (2012), namely the Galactocentric position of the Sun at  $R_\odot = 8.5$  kpc and the velocity of the local standard of rest as  $v_{LSR} = 220 \text{ km s}^{-1}$ .

## 3 NUMERICAL METHODS AND SIMULATIONS

We tested for stability over time of the Galactic stellar halo density distribution  $\rho$ , velocity dispersion  $\sigma$ , and anisotropy  $\beta$  profiles, setting them up to initially match the observations of Kafle et al. (2012). We ran simulations for 10 Gyr using  $2.24 \times 10^5$  particles in the Flynn et al. (1996) Galactic potential as described in Section 2. The stellar velocities were initially randomly drawn from Gaussian distributions and set up in a spherical non-rotating configuration. The density profile (Fig. 2) followed the double power law assumed by Kafle et al. (2012), as observed by Watkins et al. (2009) and Deason et al. (2011) where  $\rho \propto R_{GC}^{-\alpha}$  with  $\alpha = 2.4$  at  $R_{GC} \leq 27$  kpc and  $\alpha = 4.5$  at  $R_{GC} > 27$  kpc (red crosses with red fit line). Very interestingly, Deason et al. (2014) found recently a striking drop in the stellar density profile, with  $\alpha = 6$  at 50 kpc and  $\alpha = 6-10$  out to 100 kpc. Although the stellar distribution of our simulations was truncated at 500 kpc and 0.1 kpc, we do not include the most recently found drop in stellar density as it would have negligible effects on the stability of the system at much smaller radii near 17 kpc.

The initial velocity dispersions profiles are shown in the upper panel of Fig. 3.

Our simulations are of tracer stars in a fixed Galactic potential and the stars did not interact. The stellar orbits were integrated using a Runge–Kutta scheme control (Press, Flannery & Teukolsky 1986) with a 0.01 Gyr (adaptive) stepsize over a period of 10 Gyr, and the density  $\rho$ , velocity dispersion  $\sigma$ , and anisotropy  $\beta$  profiles of the particles as functions of  $R_{GC}$  were determined at 2 Gyr intervals.

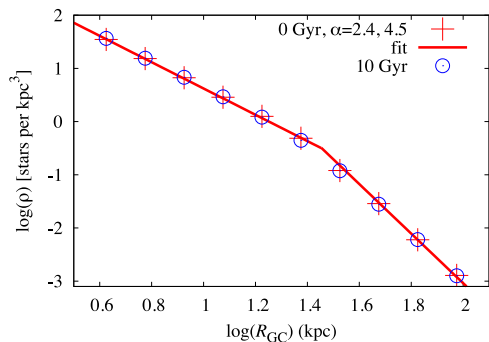


**Figure 2.** Radial density  $\rho$  profile of simulated halo stars. The initial density at 0 Gyr is the broken power law assumed by Kafle et al. (2012) (as observed by Watkins et al. 2009; Deason et al. 2011), where  $\rho \propto R_{\text{GC}}^{-\alpha}$  and  $\alpha = 2.4$  at  $R_{\text{GC}} \leq 27$  kpc and  $\alpha = 4.5$  at  $R_{\text{GC}} > 27$  kpc (red crosses with red fit line). The profile is plotted at 0 and 10 Gyr (blue circles), showing the stability of  $\rho$  as we see negligible change between the initial and final states. The break radius at which the two power laws meet is  $R_{\text{GC}} \approx 27$  kpc, or  $\log(R_{\text{GC}}) \approx 1.43$  kpc.

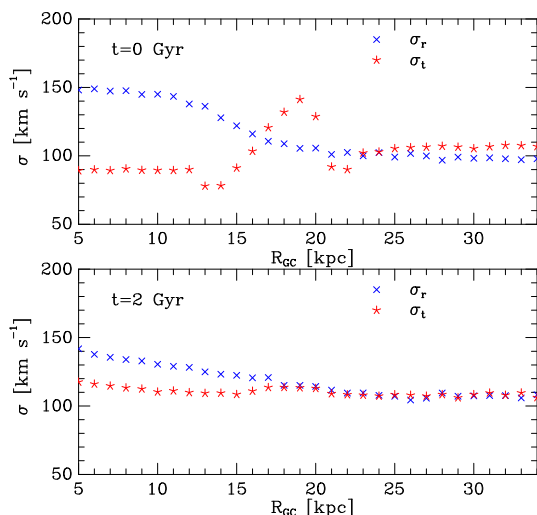


**Figure 3.** Upper panel displays the initial velocity dispersion  $\sigma$  profile from Kafle et al. (2012). Radial and tangential velocity dispersions,  $\sigma_r$  (blue crosses) and  $\sigma_t$  (red asterisks) ( $\text{km s}^{-1}$ ), respectively, are plotted as a function of distance from the Galactic centre,  $R_{\text{GC}}$  (kpc). The lower panel shows the  $\sigma$  profiles after 2 Gyr. The initial turnover features at  $R_{\text{GC}} \approx 17$  kpc in the model halo disappear within 0.02 Gyr and the new  $\sigma$  profiles remain stable in the simulations.

We found that the  $\rho$  profile was stable over the 10 Gyr simulation, as seen in Fig. 2 when comparing the negligible changes between the initial (red crosses) and final (blue circles) profiles. Unlike the stable  $\rho$  profile, the initial Kafle et al. (2012)  $\sigma$  profiles as seen in the top panel of Fig. 3 quickly relaxed to a new state, appearing in the lower panel of Fig. 3, which was stable over the remaining simulation time. Fig. 4 shows that the initial profile was quickly changed within the first 0.02 Gyr (top-right panel of Fig. 4). By 0.1 Gyr (lower-right panel of 4), relaxation had occurred and the new  $\sigma$  profiles were stable over the remaining 8 Gyr. Similarly, the initial feature in  $\beta$  disappeared and the profile remained stable during the rest of the simulation. In addition, we tested variations in the initial conditions which were consistent with the boundaries set by the error bars of the Kafle et al. (2012) determinations of sigma

versus  $R_{\text{GC}}$ . In each test, the results remained similar, showing the outcome is not dependent on one unique choice of initial conditions.

We experimented by initially exaggerating the feature to see if the stars would settle upon the actual model. We began the simulation with a larger dip in the  $\sigma_t$  profile, starting at a value of  $50 \text{ km s}^{-1}$  within the first 10 kpc instead of  $90 \text{ km s}^{-1}$ . All other conditions remained the same as our previous simulations. We found that the  $\sigma$  profiles flattened and the anomalous feature dissolved away. We ran the simulations with the same conditions as previously described, but with a model potential with a perfectly flat rotation curve, very similar to the one determined in Kafle et al. (2012). The results were the same as the other tests.

Thus we concluded the Milky Way's  $\sigma$  and  $\beta$  profiles are in a transient phase, and the observed features at 17 kpc will smooth away within a few ten million years.

#### 4 SUMMARY AND CONCLUSIONS

We tested the kinematic model of the Galactic halo proposed by Kafle et al. (2012), by directly integrating particles in the Flynn et al. (1996) 3D model of the Galactic potential, under the assumption of an initial Gaussian velocity distribution. We found that the particles relaxed quite quickly from the initial profiles observed by Kafle et al. (2012). The features at 17 kpc, most prominently seen in the anisotropy  $\beta$  profile as the steep decline reaching minimum at  $R_{\text{GC}} = 17$  kpc and the sharp rise within a few kpc, dissolved after 0.02 Gyr. We propose that this feature in the Milky Way's velocity dispersion  $\sigma$  and anisotropy  $\beta$  profiles is in a transient phase, and will flatten within a few ten million years.

Observational studies have shown that stellar inhomogeneities and substructures exist in the halo, such as the Virgo overdensity (Jurić et al. 2008) and Sagittarius stellar stream (Ibata, Gilmore & Irwin 1994), which are presumably remnants of merging satellites. Kafle et al. (2012) found that masking these two substructures did not significantly change their modelled profiles, although many underlying stellar structures yet undetected are likely to exist, such that may or may not disrupt flat profiles and lead to temporary anomalous features. Such stellar structures are testable with simulations of halo formation around disc galaxies. Deason et al. (2013) used results from such simulations to show that shell-like structures in the radial velocities of halo stars are tightly related to the furthest orbital distance of stars left over from accreted satellites.

Another possibility could be that the features in the profiles reflect underlying properties of the halo. Carollo et al. (2007) found a prograde inner halo and a retrograde more metal-poor outer halo; and Carollo et al. (2010) and de Jong et al. (2010) found the transition between such halo components to lie between  $15 < R_{\text{GC}}/\text{kpc} < 20$ , which is the location of the feature in the Kafle et al. (2012)  $\sigma$  and  $\beta$  profiles. In contrast to stellar substructures, the presence of a dual halo has been debated for and against (Schönrich, Asplund & Casagrande 2011; Beers et al. 2012; Fermi & Schönrich 2013; Schönrich, Asplund & Casagrande 2014). Despite the suggested explanations, the origins of (or combination thereof) such transient features in the halo remain unclear.

Alternatively, it is possible that the features in the  $\sigma$  and  $\beta$  profiles are due to the broken power-law stellar density distribution  $\rho$  adopted by Kafle et al. (2012), as this function is marginalised over when determining the stellar velocity dispersions. We plan to repeat similar simulations to the current paper using the more plausible density of the alpha-beta-gamma profile of Zhao (1996), which is a double power law but smooth.

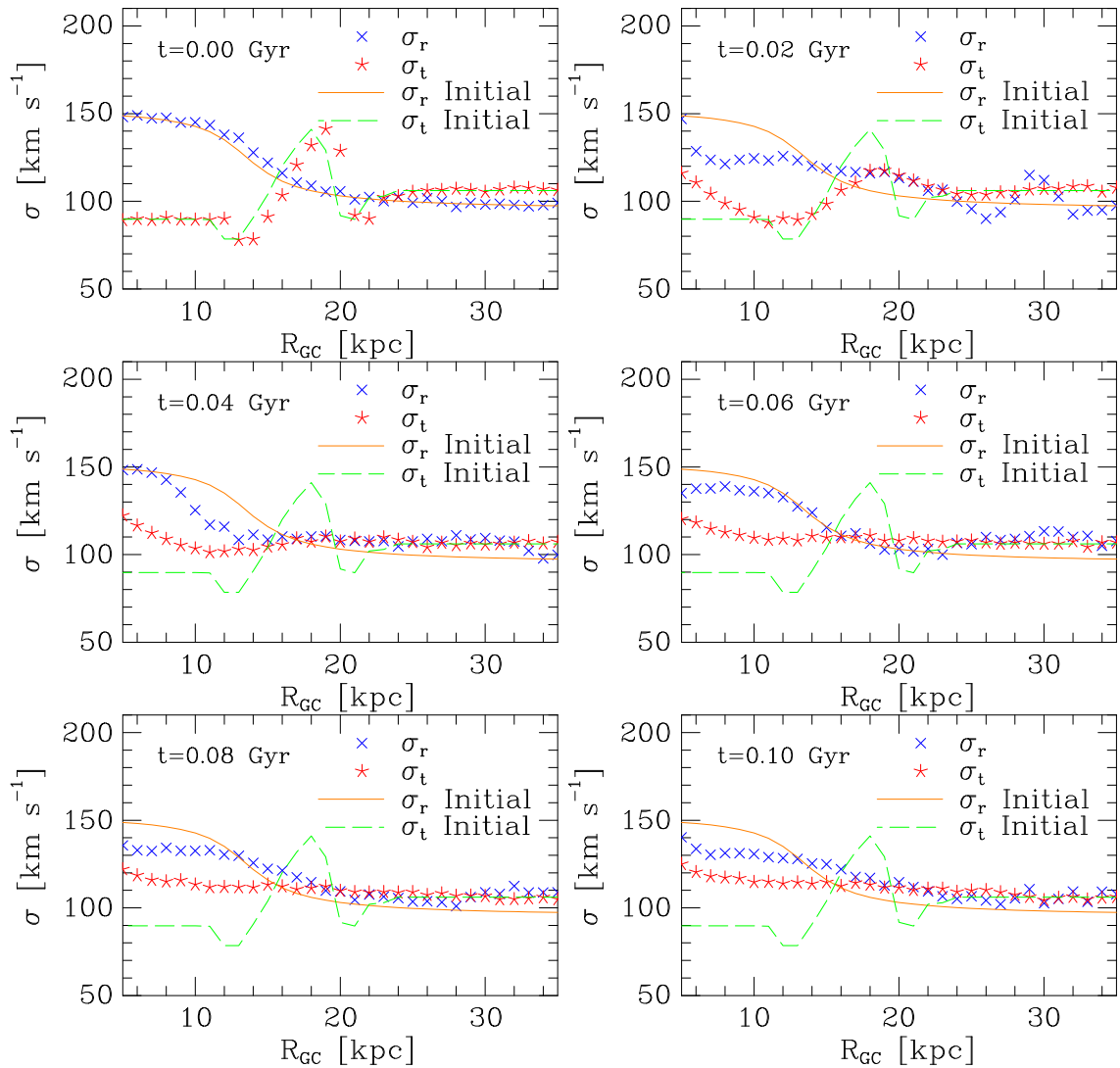


**Figure 4.** Similar to Fig. 3, but shown over the first 0.1 Gyr in the simulation. Radial and tangential velocity dispersions,  $\sigma_r$  (blue crosses) and  $\sigma_t$  (red asterisks) ( $\text{km s}^{-1}$ ), are plotted as a function of distance from the Galactic Centre,  $R_{\text{GC}}$  (kpc). The  $\sigma$  profiles are plotted every 0.02 Gyr as indicated in the top left corner of each panel. The model input  $\sigma$  profiles, as observed by Kafle et al. (2012), are plotted in each panel as the orange line ( $\sigma_r$ ) and the green dashed line ( $\sigma_t$ ). The  $\sigma_r$  and  $\sigma_t$  profiles change within the first 0.02 Gyr (top-right panel). After 0.1 Gyr, the profiles have relaxed (lower-right panel) and change negligibly over the remainder of the simulation.

In order to find what causes the features in the Galactic kinematic profiles as interpreted by Kafle et al. (2012), we plan to set up a complete library of dynamically stable haloes in the adopted Milky Way potential. The library will be particularly useful to compare with the large amounts of new data anticipated from surveys such as *Gaia* and LAMOST.

## ACKNOWLEDGEMENTS

SAB is grateful for the funding provided by the Finnish Cultural Foundation and the Turku University Foundation and for the hospitality of the Centre for Astrophysics and Supercomputing at Swinburne University of Technology where the majority of this research was carried out. SAB thanks the Emil Aaltonen Foundation and StarryStory Foundation for travel funding. The authors give special thanks to Prajwal Kafle and HongSheng Zhao for many helpful discussions, comments, and suggestions.

## REFERENCES

- Aihara H. et al., 2011, *ApJS*, 193, 29  
 Beers T. C. et al., 2012, *ApJ*, 746, 34  
 Binney J., Tremaine S., 2008, *Galactic Dynamics*, 2nd edn. Princeton Univ. Press, Princeton, NJ  
 Bovy J., Rix H.-W., 2013, *ApJ*, 779, 115  
 Carollo D. et al., 2007, *Nature*, 450, 1020  
 Carollo D. et al., 2010, *ApJ*, 712, 692  
 de Jong J. T. A., Yanny B., Rix H.-W., Dolphin A. E., Martin N. F., Beers T. C., 2010, *ApJ*, 714, 663  
 Deason A. J., Belokurov V., Evans N. W., 2011, *MNRAS*, 416, 2903  
 Deason A. J., Belokurov V., Evans N. W., An J., 2012, *MNRAS*, 424, L44  
 Deason A. J., Belokurov V., Evans N. W., Johnston K. V., 2013, *ApJ*, 763, 113  
 Deason A. J., Belokurov V., Koposov S. E., Rockosi C. M., 2014, *ApJ*, 787, 30  
 Fermani F., Schönrich R., 2013, *MNRAS*, 432, 2402  
 Flynn C., Sommer-Larsen J., Christensen P. R., 1996, *MNRAS*, 281, 1027  
 Helmi A., 2008, *A&AR*, 15, 145

- Ibata R. A., Gilmore G., Irwin M. J., 1994, *Nature*, 370, 194  
Jurić M. et al., 2008, *ApJ*, 673, 864  
Kaffe P. R., Sharma S., Lewis G. F., Bland-Hawthorn J., 2012, *ApJ*, 761, 98  
King C., III Brown W. R., Geller M. J., Kenyon S. J., 2015, preprint ([arXiv:e-prints](#))  
Miyamoto M., Nagai R., 1975, *PASJ*, 27, 533  
Press W. H., Flannery B. P., Teukolsky S. A., 1986, *Numerical Recipes. The Art of Scientific Computing*. Cambridge Univ. Press, Cambridge, p. 554  
Sandage A., 1986, *ARA&A*, 24, 421  
Schönrich R., Asplund M., Casagrande L., 2011, *MNRAS*, 415, 3807  
Schönrich R., Asplund M., Casagrande L., 2014, *ApJ*, 786, 7  
Sirko E. et al., 2004, *AJ*, 127, 914  
Sommer-Larsen J., Flynn C., Christensen P. R., 1994, *MNRAS*, 271, 94  
Sommer-Larsen J., Beers T. C., Flynn C., Wilhelm R., Christensen P. R., 1997, *ApJ*, 481, 775  
Thom C. et al., 2005, *MNRAS*, 360, 354  
Watkins L. L. et al., 2009, *MNRAS*, 398, 1757  
Xue X.-X. et al., 2011, *ApJ*, 738, 79  
Zhao H., 1996, *MNRAS*, 278, 488

This paper has been typeset from a  $\text{\TeX}/\text{\LaTeX}$  file prepared by the author.